

Climate of the Past Discussions is the access reviewed discussion forum of *Climate of the Past*

Holocene climate change in Central and Eastern Asia

A. Dallmeyer et al.

Contribution of oceanic and vegetation feedbacks to Holocene climate change in Central and Eastern Asia

A. Dallmeyer¹, M. Claussen^{1,2}, and J. Otto^{1,3}

¹Max Planck Institute for Meteorology, Hamburg, Germany

²Meteorological Institute, Klima Campus, University Hamburg, Germany

³International Max-Planck-Research School, Hamburg, Germany

Received: 23 September 2009 – Accepted: 5 October 2009 – Published: 21 October 2009

Correspondence to: A. Dallmeyer (anne.dallmeyer@zmaw.de)

Published by Copernicus Publications on behalf of the European Geosciences Union.

Title Page

Abstract

Introduction

Conclusions

References

Tables

Figures

◀

▶

◀

▶

Back

Close

Full Screen / Esc

Printer-friendly Version

Interactive Discussion



Abstract

The impact of vegetation-atmosphere and ocean-atmosphere interactions on the mid- to late Holocene climate change as well as their synergy is studied for different regions in Central and Eastern Asia (60–140° E, 0–55° N), giving consideration to the large climatic and topographical heterogeneity in that area. With main focus on the Asian monsoon, we concentrate on both, temperature and precipitation changes. For our purpose, we analyze a set of coupled numerical experiments, performed with the Earth system model ECHAM5/JSBACH-MPIOM under present-day and mid-Holocene (6 k) orbital configurations (Otto et al., 2009). Like expected, the temperature change caused by the insolation forcing reveals an enhanced seasonal cycle, with a pronounced warming in summer (0.7 K) and autumn (1 K) and a cooling in the other seasons (spring: –0.8 K; winter –0.5 K). Most of this change can be attributed to the direct response of the atmosphere, but the ocean, whose reaction has a lagged seasonal cycle (warming in autumn and winter, cooling in the other seasons), strongly modifies the signal. The simulated contribution of dynamic vegetation is small and most effective in winter, where it slightly warms the near-surface atmosphere (≈ 0.05 K). Concerning the precipitation, the most remarkable change is the postponement and enhancement of the Asian monsoon (0.27 mm/d in summer, 0.23 mm/d in autumn), mainly related to the direct atmospheric response. On regional average, the ocean (ca. 0.05 mm/d) amplifies the direct effect, but tends to weaken the East Asian summer monsoon and strongly increases the Indian summer monsoon rainfall rate (0.68 mm/d). The influence of dynamic vegetation and synergy effects on precipitation is comparatively small.

1 Introduction

The Asian monsoon is the most complex and strongest monsoon system of the world, affecting human life since the first settlement in that region (Clift and Plumb, 2008). It

CPD

5, 2351–2389, 2009

Holocene climate change in Central and Eastern Asia

A. Dallmeyer et al.

Title Page

Abstract

Introduction

Conclusions

References

Tables

Figures



Back

Close

Full Screen / Esc

Printer-friendly Version

Interactive Discussion



Holocene climate change in Central and Eastern Asia

A. Dallmeyer et al.

[Title Page](#)[Abstract](#)[Introduction](#)[Conclusions](#)[References](#)[Tables](#)[Figures](#)[Back](#)[Close](#)[Full Screen / Esc](#)[Printer-friendly Version](#)[Interactive Discussion](#)

consists of two nearly independent but also interacting monsoon systems, namely the East Asian and the Indian monsoon, and includes processes in the tropics as well as in the mid-latitudes (Lau et al., 2000). Monsoon systems are primarily driven by the seasonal differential heating between continents and oceans and the related land-sea temperature and pressure gradients. Their strength and the location of major monsoon precipitation, however, are also largely influenced by moist processes (Webster et al., 1998). Thus, each modification, that has an impact on the hydrological cycle, energy storage or exchange between land, ocean and atmosphere, affects the monsoon circulation, its onset times and duration (Yasunari et al., 2006). This includes external forcings, such as changes in insolation, as well as interactions between the different components of the climate system, which might also have a strong influence on the regional climate and impose a large intraseasonal to multi-centennial variability on the system.

Paleoreconstructions reveal significant changes of the monsoon intensity during the Holocene. Around 6000 years before present (6 k) the African as well as the Asian monsoon likely penetrated further inland, implying a wetter climate (e.g. Winkler and Wang, 1993; Kohfeld and Harrison, 2000; Ge et al. 2007; Maher, 2008) and a change in the vegetation distribution (e.g. Jolly et al., 1998; Yu et al., 2000). Early modelling studies related this enhancement of the monsoons to the impact of changing insolation on climate (e.g. Kutzbach and Otto-Bliesner, 1982; Harrison et al., 1998). Due to the variations in the Earth's orbit (mainly the precessional cycle), perihelion was reached in September (6 k) instead of January at present time, yielding an increase of summer and decrease of winter insolation in the Northern Hemisphere relative to today (Berger, 1978). The seasonal cycle was enhanced in the Northern and reduced in the Southern Hemisphere, affecting the cross equatorial ocean-land temperature gradient and thereby the monsoon flows. However, modelling studies just focusing on orbital forcing tend to underestimate the monsoon expansion and associated increase of rainfall (Joussaume et al., 1999). More recently, research studies also consider ocean and/or land interactions by performing coupled model simulations. Whereas oceanic feed-

Holocene climate change in Central and Eastern Asia

A. Dallmeyer et al.

Title Page

Abstract

Introduction

Conclusions

References

Tables

Figures

◀

▶

◀

▶

Back

Close

Full Screen / Esc

Printer-friendly Version

Interactive Discussion



backs seem to further enhance the North African monsoon (Kutzbach and Liu, 1997; Braconnot et al., 2000; Liu et al., 2004), contradictions exist about the impact of the ocean on the Asian monsoon. Several climate modelling studies report an increase of precipitation attributed to the ocean coupling (Hewitt and Mitchell, 1998; Braconnot et al., 2000; Wei and Wang, 2003). Other model results rather suggest a negative oceanic contribution to the Holocene precipitation change, i.e. a suppression of the Asian monsoon due to interactive ocean (Voss and Mikolajewicz, 2001; Liu et al., 2004 (for 11 k); Ohgaito and Abe-Ouchi, 2007; Li and Harrison, 2008).

Feedback studies concerning the role of the vegetation in Holocene climate change have mostly been applied to the African monsoon region (e.g. Claussen and Gayler, 1997; Broström et al., 1998; Irizarry-Ortiz et al., 2003; Levis et al., 2004; Hales et al., 2006). Nevertheless, some studies include or even focus on the Asian monsoon (e.g. Claussen, 1997; Texier et al., 2000; Wang, 1999; Diffenbaugh and Sloan, 2002; Li and Harrison, 2009). All model results agree, that vegetation and land-surface feedbacks could have enhanced the orbital-induced monsoon change during the Holocene.

To determine the contribution of the land-atmosphere and ocean-atmosphere interactions as well as their synergy to the climate change between the mid-Holocene (6 k) and present-day (pre-industrial climate) we analyse a set of numerical experiments, performed by Otto et al. (2009). They used a coupled atmosphere-ocean-vegetation model and applied a factor-separation technique (Stein and Alpert, 1993) to isolate the impact of different feedbacks on Holocene climate change in the northern latitudes. Following the methods of Otto et al. (2009) we repeat their study for Central and Eastern Asia (60–140° E, 0–55° N), focussing on the Asian monsoon region. Furthermore, we analyse all seasons separately.

After a short description of the model and the analysis methods in Sect. 2, we discuss the simulated climate and land-cover differences between mid-Holocene and present-day (Sect. 3). The contributions of land-atmosphere and ocean-atmosphere interactions as well as their synergy are further examined in Sect. 4.

2 Methods

2.1 Model and experiments

The results of this study are based on numerical experiments, performed by Otto et al. (2009) with the Earth system model ECHAM5-JSBACH/MPIOM, developed at the Max-Planck-Institute for Meteorology. In this model, the atmosphere is represented by ECHAM5 (Roeckner et al., 2003), extended with the land-surface scheme JSBACH (Raddatz et al., 2007). The model was run with the spectral resolution T31 ($\approx 3.75^\circ$) and 19 vertical levels, following a hybrid sigma-pressure system. JSBACH includes the dynamic vegetation module of Brovkin et al. (2009). For the ocean, MPIOM (Jungclaus et al., 2006) is used at a horizontal resolution of $\approx 3^\circ$ and 40 vertical levels.

The models have been tested against observation and reanalysis data. They capture the major structure of global and regional climate. A detailed comparison of ECHAM5 model output (resolution T63L31) and observations for the Central and East Asian region is presented by Cui et al. (2006). The simulated climate in our coupled control run does not substantially differ, although the deviation to the observed climate might be more pronounced due to the coarse resolution we chose (Roeckner et al., 2006).

The experimental set-up was designed to separate the contribution of the ocean-atmosphere, the vegetation-atmosphere interaction and their synergy from the total climate change between mid-Holocene (6 k) and present-day (0 k) by applying the factor-separation technique (Stein and Alpert, 1993). Altogether, eight experiments were undertaken: four with present-day orbital configuration (set 0 k), four with mid-Holocene orbit (set 6 k). Each set contains a control-run, performed with the atmosphere-ocean-vegetation model (AOV), two simulations with the atmosphere either coupled to the vegetation or the ocean (AV and AO, respectively) and an atmosphere-only run (A). In these experiments, the non-interactive components were prescribed as boundary conditions from the present-day runs. Thereby, the ocean (in the experiments AV_{6k} , AV_{0k} , A_{6k} and A_{0k}) was integrated as monthly mean values of SST and sea-ice, taken from the present-day run AOV_{0k} . The vegetation (in AO_{6k} , AO_{0k} , A_{6k} and A_{0k}) was pre-

Holocene climate change in Central and Eastern Asia

A. Dallmeyer et al.

Title Page

Abstract

Introduction

Conclusions

References

Tables

Figures



Back

Close

Full Screen / Esc

Printer-friendly Version

Interactive Discussion



Holocene climate change in Central and Eastern Asia

A. Dallmeyer et al.

Title Page

Abstract

Introduction

Conclusions

References

Tables

Figures

◀

▶

◀

▶

Back

Close

Full Screen / Esc

Printer-friendly Version

Interactive Discussion



scribed as fraction of land cover type per grid-box. Values were taken from AOV_{0k} for the experiments AO and from AV_{0k} for the atmosphere-only runs. Atmospheric composition was fixed at pre-industrial values in all simulations, e.g. CO_2 concentration was set to 280 ppm. All simulations were brought to equilibrium before they were running for another 600 yr in total. In the runs AV, AO and A, the ocean and/or vegetation were prescribed every 120 yr, so that the whole simulation is divided into five periods. The results of this study are based on seasonal means of all periods (i.e. 600 yr-mean). Further information on the setup of experiments is given in Otto et al. (2009).

2.2 Analysis methods

Following the factor-separation technique (Stein and Alpert, 1993), the contribution of the different components and feedbacks to the climate change between mid-Holocene and present-day (pre-industrial) climate are determined as:

Total climate change:

$$\Delta AOV = AOV_{6k} - AOV_{0k}$$

Direct response of the atmosphere:

$$\Delta A = A_{6k} - A_{0k}$$

Vegetation feedback:

$$\Delta V = (AV_{6k} - AV_{0k}) - (A_{6k} - A_{0k})$$

Ocean feedback:

$$\Delta O = (AO_{6k} - AO_{0k}) - (A_{6k} - A_{0k})$$

Synergy:

$$\Delta S = \Delta AOV - \Delta A - \Delta O - \Delta V$$

In this study, we restrict our analysis to two climate parameters, the near-surface air temperature (2 m above ground) and precipitation. Time and spatial averaging is explained in Sects. 2.2.1 and 2.2.2, respectively.

2.2.1 Calendar

Joussaume and Braconnot (1997) show that paleo-climate model results and their interpretation strongly depend on the chosen calendar. Due to the precession of the earth, not just the seasonal insolation but also the length of the seasons change in time. Comparing seasons of the mid-Holocene with present-day's, thus, requires an

absolute time reference. Joussaume and Braconnot (1997) suggest the definition of seasons based on astronomical positions, i.e. vernal equinox, summer solstice, autumnal equinox and winter solstice. In accordance with the respective astronomical dates we calculate the seasonal averages for 6 k and 0 k from daily model output. However, to facilitate the comparison of our results with previous studies, which are usually based on present-day model (meteorological) calendar (e.g. summer=JJA), we shifted the seasons backwards by three weeks. The day, each season starts at, as well as the length of the seasons is summarized in Table 1.

2.2.2 Regions

Central and Eastern Asia (60–140° E, 0–55° N) is a region with strong climatic and orographic contrasts. Affected by different circulation systems (Indian and East Asian monsoon, mid-latitude westerlies), deserts are located close to dense vegetated area and tropical climate can be found as well as regions covered by snow for half of the year. Huge mountains and high-elevated plateaus as well as wet plains around large rivers form the landscape. It appears that these regions strongly differ with respect to their atmospheric response to the orbital forcing and with respect to the strength of the feedbacks. Furthermore, reconstructions reveal an asynchronous precipitation maximum in various parts of the Asian monsoon region (An et al., 2000), which might indicate large spatial differences in the climatic change between the mid-Holocene and today.

Therefore, we divided the region into characteristic sub-areas, based on topography and the simulated Holocene vegetation trend. A detailed description of the sub-areas is given in Table 2 and Fig. 1. Although these sub-regions seem to be small (sometimes only averaging nine grid boxes), the differences among them and the characteristic features, we used for the allocation, are robust. In addition, the results are based on a long model experiment (600 yr-averages), increasing the significance and reliability. The division of the region into smaller characteristic areas facilitates a detailed analysis of the climate change and the contribution of different feedbacks.

Holocene climate change in Central and Eastern Asia

A. Dallmeyer et al.

Title Page

Abstract

Introduction

Conclusions

References

Tables

Figures



Back

Close

Full Screen / Esc

Printer-friendly Version

Interactive Discussion



3 Main characteristics of Central and East Asian climate and land cover changes

3.1 Climate change from 6 k to present-day

The climate in Central and Eastern Asia is influenced by three different circulation systems: the East Asian monsoon, the Indian monsoon and the mid-latitude westerlies. These systems are all strongly affected by the Tibetan Plateau. They in turn originate from different climate factors and are characterized by distinct seasonal cycles. Therefore, the regional climate is very heterogeneous, with arid and desert like conditions in the northwest, a general wet southern and eastern part and an alpine climate on the elevated Tibetan Plateau.

Before discussing the climatic impact of the dynamic ocean and vegetation (next section), we describe the main characteristics of the climate and land cover changes on the basis of the coupled experiments AOV_{6k} and AOV_{0k} and compare the results with reconstructions. In our analysis we focus on precipitation as the basic parameter characterizing monsoonal influenced climates and near-surface air temperature (temperature 2 m above ground). Both variables strongly determine the vegetation distribution.

3.1.1 Near-surface air temperature (2 m)

Figure 2 shows the geographically resolved temperature change from 6 k to 0 k for each season and as annual mean. For the mid-Holocene spring, the model simulates lower near-surface air temperatures over the whole region (60–140° E, 0–55° N) compared to present-day. Maximal cooling occurs in the northern part of India (up to 2.8 K) and on the Tibetan Plateau (1.5–2 K).

Whereas summer temperature is increased in the regions north of 30° N with maximum amplitude of 3 K, the western Pacific as well as the region between 20° N and 30° N, particularly northern India and the southern rim of the Tibetan Plateau, expe-

Holocene climate change in Central and Eastern Asia

A. Dallmeyer et al.

Title Page

Abstract

Introduction

Conclusions

References

Tables

Figures



Back

Close

Full Screen / Esc

Printer-friendly Version

Interactive Discussion



rience a cooler near-surface climate under 6 k orbital conditions (up to -1.6 K). The slightly higher temperatures over South India, Indochina and the adjacent Indian Ocean are negligible (<0.5 K).

5 With the exception of some grid-boxes south west of the Tibetan Plateau, an up to 3 K temperature rise occurs in all parts of the considered region in autumn (up to 2.2 K).

For the winter season, the model results reveal lower near-surface temperatures over the continental area south of 55° N and slightly higher temperatures above the adjacent oceans. The strongest change occurs in the coastal areas and in the region south west of the Tibetan Plateau.

10 Averaged over the year, the Asian Monsoon region experiences a cooling of up to 1.5 K (northern India). Near-surface air temperatures in the other regions are slightly (<0.5 K) higher in 6 k than in 0 k. The warming becomes more pronounced in the northern latitudes.

3.1.2 Precipitation

15 The seasonal precipitation changes between mid-Holocene and present-day are illustrated in Fig. 3. One has to be careful with the interpretation of precipitation changes. Due to the differences in the length of the respective seasons between 6 k and 0 k, a higher precipitation rate per day does not necessarily indicate a higher seasonal mean. In this study, precipitation is always measured in mm/d.

20 On average, the Asian monsoon regions and adjacent oceans receive less spring precipitation (up to 1 mm/d) under 6 k orbital conditions, likely indicating a later onset of the summer monsoons. In all other parts of the region precipitation is slightly enhanced, in particular on the Tibetan Plateau, where snowfall is increased by nearly 0.5 mm/d.

25 The mid-Holocene summer climate is characterized by more precipitation (per day) than today in most parts of Central and Eastern Asia, but the difference is often smaller than 1 mm/d. The strongest change occurs at the southern rim of the Tibetan Plateau, where the steep slope of the Himalaya induces an increase in precipitation of 3–

Holocene climate change in Central and Eastern Asia

A. Dallmeyer et al.

Title Page

Abstract

Introduction

Conclusions

References

Tables

Figures



Back

Close

Full Screen / Esc

Printer-friendly Version

Interactive Discussion



4 mm/d for 6 k. In contrast, rainfall decreases in the north eastern Bay of Bengal and the East and South China Sea (up to 2 mm/d).

In autumn, the area gaining more precipitation in 6 k is expanded to the adjacent oceans. Averaged daily precipitation is especially enhanced in the Indian monsoon region (up to 2 mm/d). A reduction of rainfall rate is only apparent at some grid boxes east of the Tibetan Plateau, the northern Bay of Bengal and in the non-coastal western Pacific.

In most parts of East China wintertime precipitation is decreased in 6 k compared to present-day. The largest change on the continent occurs in the Yangtze-Plain (up to 0.7 mm/d). The northern regions and India receive slightly more precipitation. Except for the Bay of Bengal (up to -1.5 mm/d) all adjacent oceans experience an enhancement of precipitation rate (up to 1.5 mm/d).

On average, the annual precipitation rate is increased over land in 6 k (up to 1 mm/d), except for the Yangtze-Huanghe-Plain.

3.2 Land cover change from 6 k to present-day

The differences in climatic conditions for 6 k and 0 k induce large-scale land cover changes (Fig. 4). The simulated vegetation changes are assigned to four categories, namely forest, shrub, grass and non-vegetated fraction of a grid box (in the following referred to as desert fraction). Overall, Central Asia is covered by more vegetation in 6 k, although the decrease in desert fraction is mostly small, not reaching changes higher than 10%. Only the region south west of the Tibetan Plateau and the margin area of the East Asian summer monsoon experience a larger increase of vegetated area (up to 40%).

On the contrary, the desert in North Africa and Arabia is strongly reduced. In the transition zone between monsoon-influenced area and nearby desert or sparsely vegetated area, the fraction covered by any type of vegetation is controlled by rainfall. The Tibetan Plateau is a large orographic barrier, constraining a further inland penetration of the Indian and East Asia summer monsoon, whereas the African monsoon is able

Holocene climate change in Central and Eastern Asia

A. Dallmeyer et al.

Title Page

Abstract

Introduction

Conclusions

References

Tables

Figures



Back

Close

Full Screen / Esc

Printer-friendly Version

Interactive Discussion



to expand northward. Since most of the total precipitation in those regions can be attributed to the summer monsoons, changes in the amount of rain at the lee side of the Tibetan Plateau and thereby the reduction of the desert fraction must be small.

For the monsoon regions, where the moisture supply is sufficient, the model only simulates a change in the type of vegetation. In 6k, more area is covered by forest instead of shrubs and grass, particularly in the region south of and on the Tibetan Plateau as well as Eastern China. In the Indian monsoon region, part of the grass is replaced by shrubs.

Pollen analyses reveal a generally increased forest cover in the central and eastern parts of China (e.g. Ren and Beug, 2000; Ren, 2007) and a northwestward shift of the steppe-forest boundary of up to 500 km (Ren, 2007; Yu 2000) for Mid-Holocene climate. Due to the coarse resolution of the model, this shift is consistent with a westward migration of forests of just one grid-box. A northward displacement cannot be distinguished. Ren (2007) reports a decline of arboreal pollen in Northeast China (123–133° E, 40–52° N) from 6k to 0k. Although the regions do not exactly coincide, the tendency of less forest in the northeastern part of China is also apparent in the model. Pollen reconstructions from the Tibetan Plateau indicate a spatial heterogeneous vegetation trend. Many records collected on the Eastern and Southern Tibetan Plateau reveal a reduction of moisture availability and forest cover since 6k (e.g. Herzschuh et al., 2006; Shen et al., 2006; Tang et al., 1999), which are proposed to be associated with a gradual weakening of the Asian summer monsoon. However, some records also show comparably dry and even drier conditions in the mid-Holocene affecting the local vegetation composition (Zhao et al., 2009; Herzschuh et al., 2009). This inhomogeneous land cover trend is also obvious in the model results.

Given the coarse resolution of the model, the spatial distribution of the simulated vegetation changes between Mid-Holocene and present-day agrees well with the reconstructions. However, the magnitude of changes differs. Whereas reconstructions suggest a decrease in forest cover of up to 90% (Ren, 2006) our model reveals differences of <50%.

Holocene climate change in Central and Eastern Asia

A. Dallmeyer et al.

Title Page

Abstract

Introduction

Conclusions

References

Tables

Figures

◀

▶

◀

▶

Back

Close

Full Screen / Esc

Printer-friendly Version

Interactive Discussion



4 The impact of the dynamic vegetation and ocean on the climate change between 6 k and present-day

4.1 Near-surface air temperature (2 m)

4.1.1 Direct response of the atmosphere to the orbital forcing

5 Figure 5 illustrates the contribution of the ocean and vegetation feedback to the temperature change as well as the direct response of the atmosphere to the orbital forcing and their synergy as seasonal means for each defined area. Following the latitudinal differences in orbital-induced insolation change between 6 k and 0 k, the direct reaction of the atmosphere causes a more pronounced spring- and wintertime cooling in the southern areas (up to -1.8 K) than in higher latitudes ($< -0.3\text{ K}$). Exceptions are the areas along the western Pacific (YANG, INCPIN), where the atmospheric contribution is relatively small in spring. In contrast, the Bay of Bengal bordering region (BENG) as well as the Tibetan Plateau (TP) reveal a particularly large spring temperature decrease. Two different mechanisms might affect these anomalies and variations: Due to the orbital-induced decrease in temperature, the wintertime snowfall rate is enhanced in a large area between the Tibetan Plateau and the east coast of China, leading to a higher surface albedo, a reduction of absorbed solar energy and an amplification of the near-surface cooling (snow-albedo feedback). In spring, this mechanism is still acting on the Tibetan Plateau, likely creating the contrast to the surrounding areas. The anomalies in the other regions might be associated with a change in evaporation. In the northern part of India (including BENG) the latent heat flux is strongly increased (up to about 20 W/m^2 in spring) at the expense of the sensible heat flux. This leads to a more effective surface cooling in winter as well as in spring. For Indochina (INCPIN) and the Yangtze-Huanghe Plain (YANG) the relatively small temperature change in spring might reflect a decrease of evaporative cooling due to a later onset of the East Asian summer monsoon. This partly compensates the temperature decline expected from the insolation change.

10

15

20

25

Title Page

Abstract

Introduction

Conclusions

References

Tables

Figures



Back

Close

Full Screen / Esc

Printer-friendly Version

Interactive Discussion



Holocene climate change in Central and Eastern Asia

A. Dallmeyer et al.

Title Page

Abstract

Introduction

Conclusions

References

Tables

Figures



Back

Close

Full Screen / Esc

Printer-friendly Version

Interactive Discussion



The near-surface temperature difference between 6 k and 0 k in summer is strongly determined by the direct response of the atmosphere to the orbital forcing. Coincident with the latitudinal gradient of the insolation change, a temperature increase of up to 2.8 K in the northern regions and a weaker warming (ca. 0.3–0.6 K) in the southern regions is obtained. Only in the area south of the Tibetan Plateau (BENG, partly IND) the direct effect tends to diminish the near-surface temperature, likely caused by higher precipitation rates (enhanced and shifted summer monsoon) and the related evaporative cooling.

The enhancement and later retreat of the Asian summer monsoon (see Sect. 4.2) might also be responsible for the unexpected (with regard to the insolation change) distribution of the autumnal warming in the atmosphere-only runs: Despite of the negative latitudinal gradient of solar incoming radiation difference between mid-Holocene and present-day the strongest temperature rise occurs in the northern regions (up to 1.7 K in NECH) and not near the equator. The later retreat of the Asian summer monsoon is accompanied by an increase in cloudiness, resulting in a weaker net solar radiation at the surface.

4.1.2 Contribution of the dynamic ocean

The atmosphere-ocean feedback exerts a cooling in all considered parts of Asia in spring and summer, thereby amplifying the atmospheric signal in the former and counteracting the direct response in the latter of these seasons. Due to the small direct effect in the near equatorial areas, the contribution of the interactive ocean to the summer temperature change is relatively large in the Indian monsoon region. Thus, it can compensate the direct warming. However, the magnitude of the ocean induced cooling is generally small in summer as well as in spring (< -0.5 K in most areas). Only in India and on the Indochina Peninsula the springtime temperature decrease associated with the atmosphere-ocean interaction reaches large values of -1.1 K and -0.9 K, respectively. In those regions evaporation is strongly enhanced, likely causing this pronounced cooling.

Holocene climate change in Central and Eastern Asia

A. Dallmeyer et al.

Title Page

Abstract

Introduction

Conclusions

References

Tables

Figures



Back

Close

Full Screen / Esc

Printer-friendly Version

Interactive Discussion



In autumn, the contribution of the interactive ocean amplifies the direct effect and shows a warming in the same order of magnitude as the atmospheric response. It ranges from 0.13 K in IND to 0.8 K on the Tibetan Plateau. No autumnal temperature change can be attributed to the ocean in PAK.

The ocean-atmosphere interaction leads to a cooling (≈ -0.4 K) of the tropical regions (IND, INCPIN) in boreal winter, which intensifies the direct response of the atmosphere to the insolation change. This might be associated with a soil wetness anomaly generated by an ocean-induced precipitation increase in autumn, which probably leads to more evaporation and thereby a strong cooling in winter. On the other hand the ocean feedback reduces the temperature decrease, given by the atmosphere-only run, in higher latitudes (up to 0.6 K in CETP).

The oceanic response to the insolation change seems to lag the direct response by about one month, reflecting the higher thermal inertia of the water mass. This causes a shift in the seasonal cycle of the oceanic contribution compared to the atmospheric response.

4.1.3 Contribution of the dynamic vegetation

The contribution of the dynamic vegetation is small compared to the oceanic and atmospheric response, reaching at most 0.25 K on the Central Tibetan Plateau in autumn. With few exceptions it reveals a warming in higher latitudes and a cooling in the tropical regions (in particular India) during the whole year. There are different mechanisms, which might be involved in this temperature change: Overall, most of the regions are covered with more vegetation in 6 k. This is accompanied by a reduction of surface albedo and a potential warming of the near-surface air, due to more absorbed shortwave radiation at the surface. In accordance, the vegetation induced increase in temperature is particularly large in some parts of the Tibetan Plateau and in the margin area of the East Asian summer monsoon (up to 0.22 K), where the slightly further inland penetrating summer monsoon favors the occurrence of forests in 6 k. Furthermore, these regions are covered by snow in winter and spring, so that the increase in

forest fraction leads to a higher snow-masking effect and a pronounced reduction of the surface albedo in those seasons (up to 0.05). Therefore, the vegetation-induced winter and spring warming is strongest in these regions.

The slight temperature decrease in the Indian monsoon region in summer (0.1–0.2 K), and in IND and INCPIN in all seasons, are likely related to an increase of evapo-transpirational cooling of the surface due to an enlargement of the area covered by higher vegetation (shrubs instead of grass and desert).

Apart from the effect on the local energy balance the interactive vegetation leads to a change in local atmospheric dynamics. The increase in forest and vegetation cover northeast of the Tibetan Plateau warms the surface and weakens the anticyclone, which develops in autumn over the cold landmasses of northern Asia (not shown). This implies a reduction of the northeasterly flow, leading to a weaker cold-air advection to the Yangtze-Huanghe-Plain and southeastern China. Total cloud cover as well as snow fall decrease, yielding an additional warming of the near-surface atmosphere in autumn and winter. Thus, the winter-temperature increase in YANG is also relatively high (0.22 K).

In autumn, a slight decrease (<0.08 K) in 2 m-temperature is apparent in DES, RUS and NECH, probably reflecting an increase in total cloud cover and less solar radiation available at the surface.

4.1.4 Contribution of the synergy

The synergy between the ocean-atmosphere and vegetation-atmosphere feedback is small but on average positive in nearly all regions and seasons. Its contribution to the temperature change tends to be larger in the southern regions (IND, PAK, INCPIN, BENG) than in the north. The warming reaches values of up to 0.34 K in spring, 0.16 K in summer (IND), 0.18 K in autumn (BENG) and 0.2 K in winter (PAK). A noticeable cooling (up to -0.2 K) of the near-surface atmosphere associated with the synergy effect only occurs in YANG, RUS and NECH in winter.

Holocene climate change in Central and Eastern Asia

A. Dallmeyer et al.

Title Page

Abstract

Introduction

Conclusions

References

Tables

Figures



Back

Close

Full Screen / Esc

Printer-friendly Version

Interactive Discussion



4.2 Precipitation

4.2.1 Direct response of the atmosphere to the orbital forcing

The contributions of the dynamic ocean and vegetation to the precipitation change as well as the direct response of the atmosphere to the orbital forcing and their synergy are depicted in Fig. 6 as seasonal means for each defined area.

The dominant mechanism forming the monsoons is the thermal contrast between the land and the ocean. Thus, the seasonal cycle of monsoons is primary determined by the distribution of incoming solar radiation, which depends on the Earth's orbit around the sun (Webster et al., 1998; He et al., 2007). As expected, the change of the orbital parameter from 0 k to 6 k affects the simulated annual cycle of monsoon precipitation in Central and East Asia. The reduced solar energy input in spring postpones the East Asian summer and Bay of Bengal monsoon onset. Therefore less spring precipitation is received in Indochina (-0.4 mm/d), India (-0.06 mm/d), BENG (-0.15 mm/d), the Yangtze-Huanghe-Plain (-0.33 mm/d) and also in NECH (-0.04 mm/d), associated with the direct effect of the atmosphere to the insolation change.

As a consequence of the strong continental warming in summer, the large-scale circulation is modified. The upper tropospheric flow over Africa and the Central Asian continent is much more divergent in summer, except over South India and some parts of Indonesia (Fig. 7). This is related to an enhanced vertical uplift of moist air, more clouds and higher precipitation-rates in all other considered regions, in particular in the areas influenced by the summer monsoon. Whereas the East Asian monsoon is intensified and penetrates further inland (EASM $+0.41$ mm/d), the atmosphere-only run suggests less precipitation (weaker monsoon) in India (-0.4 mm/d). Due to a low-level pressure anomaly in the area between Kazakhstan and the Arabian Sea (≈ 3 hPa, Fig. 8), the low level Indian monsoon flow is slightly shifted in 6 k compared to present-day, strengthening the monsoon branch directed to the north Arabian Sea. Over Pakistan, this branch turns towards and streams along the Tibetan Plateau, resulting in more precipitation south of the Plateau (BENG: $+1.77$ mm/d). By contrast, the mon-

Holocene climate change in Central and Eastern Asia

A. Dallmeyer et al.

Title Page

Abstract

Introduction

Conclusions

References

Tables

Figures



Back

Close

Full Screen / Esc

Printer-friendly Version

Interactive Discussion



soon flow in South India and the southern Bay of Bengal is diminished. The changes in precipitation as well as OLR distribution (not shown) suggest a northward shift of the ITCZ in summer.

The atmospheric response to the orbital forcing leads to more autumn precipitation in all regions (Fig. 6), especially in the coastal areas, and less precipitation over the adjacent oceans, suggesting a later retreat of the summer monsoon system.

The change of wintertime precipitation is small in all regions. The direct effect is a decrease of precipitation in East and Northeast Asia (NECH, RUS, INCPIN, YANG), especially in the Yangtze-Huanghe-Plain (-0.25 mm/d). Due to a general orbital-induced cooling of the near-surface air layer and the accompanied high-pressure anomaly above the continent, the low level flow toward the ocean is increased, leading to both, more subsidence and less moist air advection. This reduces cloud cover and precipitation in East China. In all other regions, winter precipitation is slightly increased (up to 0.08 mm/d).

4.2.2 Contribution of the dynamic ocean

The oceanic impact on the seasonal precipitation distribution is mainly manifested in the change of evaporation and the modification of the large-scale and local circulation due to changed SSTs. Thus, lower SSTs in spring reduce evaporation. The accompanied decrease of the moist-air advection from the ocean to the continent might be responsible for the reduction of precipitation in all regions. The most affected area is the Yangtze-Huanghe-Plain (-0.15 mm/d).

In summer, the pattern of large-scale circulation change due to the interactive ocean offers a much more divergent upper-tropospheric flow above the Arabian Sea and an increased convergence above the Pacific (not shown). This collocates with a centre of enhanced evaporation in the South Arabian Sea and reduced evaporation in the East China Sea, influencing the precipitation change over the whole continent due to more water availability in the Indian and diminished water supply to the East Asian monsoon. Whereas less precipitation is received around the Tibetan Plateau (up to

Holocene climate change in Central and Eastern Asia

A. Dallmeyer et al.

Title Page

Abstract

Introduction

Conclusions

References

Tables

Figures



Back

Close

Full Screen / Esc

Printer-friendly Version

Interactive Discussion



Holocene climate change in Central and Eastern Asia

A. Dallmeyer et al.

Title Page

Abstract

Introduction

Conclusions

References

Tables

Figures

◀

▶

◀

▶

Back

Close

Full Screen / Esc

Printer-friendly Version

Interactive Discussion



–0.15 mm/d), India (+0.68 mm/d) and the north coast of the Arabian Sea (including PAK: +0.18 mm/d) experience a strong increase of rainfall-rate. This oceanic-induced strengthening of the Indian summer monsoon overcompensates the direct effect in India (IND), causing the wetter summer climate in 6 k compared to 0 k in this area. In all other regions summer precipitation is increased, as well (up to 0.12 mm/d in YANG). The interactive ocean tends to weaken the East Asian summer monsoon. However, apart from the reduction of water supply mentioned above, colder than present SSTs in the west Pacific induce a high pressure anomaly (anticyclone) and an enhanced monsoon flow onto the continent. These two mechanisms counteract and lead to small changes in the East Asian monsoon region.

Likely due to the thermal inertia of the ocean, the sea surface is warmed the most in autumn. SSTs are higher in most parts of the adjacent oceans, particularly in the north Arabian Sea. This leads to a warmer lower atmosphere and more evaporation, resulting in more water vapour in the atmosphere. These moist air masses are advected to the land, prolonging the rain period of the Indian summer monsoon (except in BENG). The most remarkable change occurs in India (+0.88 mm/d), where the ocean feedback triples the precipitation increase associated with the direct response of the atmosphere to the insolation change. In the East Asian monsoon, rainfall-rate is only weakly affected by the interactive ocean (<0.04 mm/d).

The interactive ocean mostly causes a slight decrease of precipitation in winter, partly compensating the direct effect of the atmosphere. The oceanic-induced changes are most pronounced in the area around the Tibetan Plateau (ca. –0.1 mm/d) and in YANG (–0.11 mm/d), where the atmospheric warming attributed to the ocean likely results in a decrease of cloud cover and snowfall.

4.2.3 Contribution of the dynamic vegetation

The seasonal precipitation-rates are only little affected by vegetation-atmosphere interactions. Nevertheless, the vegetation feedback mostly tends to amplify the direct response to the orbital forcing in all seasons except winter. In spring, the interactive

Holocene climate change in Central and Eastern Asia

A. Dallmeyer et al.

Title Page

Abstract

Introduction

Conclusions

References

Tables

Figures

◀

▶

◀

▶

Back

Close

Full Screen / Esc

Printer-friendly Version

Interactive Discussion



vegetation reduces precipitation in the region south of ca. 32° N (up to -0.04 mm/d in BENG). Everywhere else precipitation as well as evaporation is increased, especially at the center of the Tibetan Plateau (0.08 mm/d). The slightly lower temperatures in India are accompanied by a high-pressure anomaly, yielding a low level flow from the continent to the ocean. Thereby, the monsoon flow is inhibited and cloud cover as well as precipitation is reduced.

Likely associated with the enlargement of area covered by higher vegetation (shrubs, forest instead of grass and desert) and an increase of evapotranspiration in summer and autumn, the precipitation-rate is intensified in the Indian monsoon region by up to 0.12 mm/d (IND for autumn). Precipitation in the northernmost regions (NECH, RUS) is also slightly enhanced (up to 0.04 mm/d). In YANG, the vegetation feedback tends to weaken the large-scale precipitation (ca. -0.04 mm/d in autumn).

The contribution of the vegetation to the wintertime precipitation change is very small. The model results suggest more precipitation in India (0.007 mm/d) and in the regions north of 40° N (up to 0.015 mm/d). Less precipitation is received in the other regions, particularly in BENG and on the Tibetan Plateau, where snowfall is decreased as a consequence of the interactive vegetation.

4.2.4 Contribution of the synergy

In spring, the synergy between the ocean-atmosphere and vegetation-atmosphere feedback leads to more precipitation in the regions south of 32° N (up to 0.07 mm/d in BENG) and less precipitation in EASM as well as on the Central Tibetan Plateau (up to -0.05 mm/d). Thus, it counteracts the direct response of the atmosphere to the insolation change.

Compared to the other components, the synergy effect is very small in summer (below 0.05 mm/d), mostly reaching magnitudes only half as large as the vegetation feedback. Its contribution to autumn precipitation change is also negligible, except for IND and BENG, where it shows values of -0.11 mm/d and -0.08 mm/d, respectively.

In winter, the synergy leads to an increase in precipitation (up to 0.05 mm/d in

BENG) in most regions, but INCPIN and EASM (both ca. -0.01 mm/d) reveal a slight decrease of precipitation-rate.

5 Summary and discussion

The impacts of interactive ocean and vegetation on the climate change from mid-Holocene to present-day have been investigated for Central and East Asia (60 – 140° E, 0 – 55° N) by applying the factor separation technique (Stein and Alpert, 1993) on a set of numerical experiments. We focus especially on the Asian summer monsoon region. In summary, the regional mean temperature change over the land for each season is depicted in Fig. 9a. Following the general differences in incoming solar radiation, the region experiences an overall cooling of ≈ 0.8 K, on average, in spring and a comparable warming (ca. 1 K) in autumn. In summer, only the subtropical parts (north of 30° N) are strongly warmed, causing an averaged temperature rise of ca. 0.7 K. On the contrary, the decrease of winter temperature is most apparent in the tropical regions, whereas the region north of 50° N experiences a warming (see Fig. 2). Nevertheless, the regional mean winter temperature difference is negative (ca. -0.5 K).

Most of the temperature change in Central and East Asia can be attributed to the direct response of the atmosphere to the orbital forcing. Its distribution is strongly determined by the modified seasonal cycle, locally influenced by the snow albedo effect and changes in evaporation. The ocean, however, alters the magnitude of the temperature change. Due to the larger thermal inertia compared to the atmosphere, the ocean-induced response lags the insolation forcing by one month to one season. Therefore, the ocean feedback leads to an additional warming (on average 0.35 K) in autumn and an additional cooling (on average -0.23 K) in spring. In summer and winter it counteracts the direct effect by -0.17 K and 0.18 K, respectively. Due to the shifted seasonal cycle of the ocean contribution, the ocean modifies the thermal influence of the Tibetan Plateau. The Tibetan Plateau is a large elevated heat source in summer (March to October) and a weak heat sink in winter, exerting a strong impact on

Holocene climate change in Central and Eastern Asia

A. Dallmeyer et al.

Title Page

Abstract

Introduction

Conclusions

References

Tables

Figures



Back

Close

Full Screen / Esc

Printer-friendly Version

Interactive Discussion



the Asian climate and the regional energy balance (Wu et al., 2006, Liu et al., 2007). By cooling the Plateau in summer and warming it in autumn, the ocean attenuates the magnitude of the heat source at the beginning of the monsoon season and likely postpones the monsoon onset. This affects the climate in the whole region.

Although the interactive vegetation and synergy term play a role in some seasons and regions, the averaged contribution to the temperature change (6 k–0 k) is rather small (<0.05 K). Both show a warming in all seasons. The vegetation feedback acts in the northern regions (Tibetan Plateau, and north) by affecting the albedo, whereas in the southern regions the hydrological aspect (changes in evapotranspiration) seems to be more important.

Otto et al. (2009) also investigated the contribution of atmosphere-vegetation and atmosphere-ocean feedbacks to the near-surface air temperature change between mid-Holocene and present-day. They focused on the region north of 40° N. Despite of the very different circulation systems determining the climate in Central Asia and in the northern latitudes, respectively, the influence of the feedbacks and the direct response of the atmosphere to the orbital forcing are on average similar. The temperature change in both regions is mostly associated with the direct effect, altered by the interactive ocean. However, the atmospheric contribution is much more relevant in the monsoon region and clearly determines the sign of the seasonal temperature change in Central and Eastern Asia. On the contrary, the ocean feedback affects decisively the northern latitude temperature signal, leading to a winter warming (≈ 0.3 K) despite of less insolation in 6 k. The vegetation feedback rather plays a minor role in both regions.

As expected, considering the orbital-induced insolation change, the temperature decrease in spring is more pronounced in the monsoon regions, whereas the summer warming is twice as large in the northern latitudes. In autumn, the region north of 40° N experiences a stronger temperature increase (ca. 1.8 K) than the Asian monsoon region, although the positive insolation change is more pronounced in the tropics. This partly reflects the large influence of the ocean-atmosphere feedback on the northern latitude autumnal warming. On the other hand, the Central and East Asian temperature

Holocene climate change in Central and Eastern Asia

A. Dallmeyer et al.

Title Page

Abstract

Introduction

Conclusions

References

Tables

Figures

◀

▶

◀

▶

Back

Close

Full Screen / Esc

Printer-friendly Version

Interactive Discussion



change is strongly affected by evaporative and radiational cooling due to an enhanced summer monsoon activity.

Concerning precipitation, the strongest change is the postponement and strengthening of the summer monsoon season, causing a decrease of pre-monsoonal (spring) precipitation and an increase in summer and autumn rainfall. Whereas the East Asian monsoon is enhanced, the Indian monsoon flow is rearranged, leading to much more precipitation at the western and northern coast of the Arabian Sea and the southern rim of the Tibetan Plateau. Figure 9b shows the regionally averaged precipitation change from 6 k to 0 k over land. Most of the averaged summer and autumn precipitation increase can be attributed to the direct response of the atmosphere to the insolation change (0.2 mm/d and 0.17 mm/d, respectively). Both, the vegetation (≈ 0.01 mm/d) and the ocean (≈ 0.05 mm/d) further amplify the higher precipitation rate (on average), mostly caused by an enhancement of evaporation and a better water recycling. Furthermore, changing SSTs in the coupled ocean experiments has a strong influence on the large-scale circulation and modifies the tropospheric divergence pattern. However, the regional averaged contribution of the interactive ocean is strongly determined by the increase of precipitation in India. The East Asian monsoon rather tends to weaken due to the ocean-atmosphere interaction. The springtime precipitation reduction (on average -0.06 mm/d) is driven similarly by the atmospheric response and the ocean feedback. In contrast, the slight regional averaged decrease of the precipitation rate in winter (-0.03 mm/d) is mostly related to the dynamic ocean. The vegetation feedback is small in both seasons.

The simulated overall climate change by and large agrees with the reconstructions, which suggest an increase in summer temperature of 1–5 K, depending on the latitude (Ge et al., 2007). The magnitude of the warming, however, is smaller in the model. In addition, our results do not show a winter warming as reconstructions reveal. This might be a consequence of the underestimated simulated vegetation change for that region. Although our model captures the main vegetation trend, the modelled change in forest cover is much smaller than found in the reconstructions (e.g. Ren, 2007).

Holocene climate change in Central and Eastern Asia

A. Dallmeyer et al.

Title Page

Abstract

Introduction

Conclusions

References

Tables

Figures



Back

Close

Full Screen / Esc

Printer-friendly Version

Interactive Discussion



Therefore, the model might underestimate the vegetation feedback.

A comparison of our results with previous model studies is difficult, because neither the factor separation technique nor a consequent feedback study, including vegetation and ocean, have been applied to climate model experiments for the Asian monsoon region. Furthermore, most studies concentrate on the summer season. If applicable, our results are in line with recent studies. The response of the atmosphere reveals the same spatial distribution and magnitude of summer precipitation change as in Ohgaito and Abe-Ouchi (2007) and also corresponds with the results of Li and Harrison (2008), although their model suggests a larger change. Our simulated temperature trend is also similar to these studies. Concerning the ocean feedback, our results confirm the conclusion, that the ocean rather suppresses the direct atmospheric response in the summer season (Liu et al., 2003; Ohgaito and Abe-Ouchi, 2007; Li and Harrison, 2008). But they do not show an overall ocean-induced weakening of the summer monsoon. On average, the precipitation is enhanced on the continent, in summer as well as in autumn. The contribution of interactive vegetation in our model is weaker than in other studies (e.g. Diffenbaugh and Sloan, 2002; Zheng et al., 2004). In particular, it does not capture the large vegetation-induced winter warming.

Although our results provide a broad insight into the feedback mechanism, which might be involved in the Holocene Central Asian climate change, the magnitude of the feedbacks still requires further discussion. A detailed comparison with reconstructions is necessary, but only possible in numerical experiments with higher spatial resolution, revealing a better representation of the topography and land cover change.

Acknowledgement. This study is part of the HOLOCV-project (priority program: INTERDY-NAMIK), funded by the German Research Foundation (DFG). The authors want to thank anonymous reviewers for their helpful comments.

The service charges for this open access publication have been covered by the Max Planck Society.

Holocene climate change in Central and Eastern Asia

A. Dallmeyer et al.

Title Page

Abstract

Introduction

Conclusions

References

Tables

Figures



Back

Close

Full Screen / Esc

Printer-friendly Version

Interactive Discussion



References

- An, Z., Porter, S. C., Kutzbach, J. E., Wu, X., Wang, S., Liu, X., Li, X., and Zhou, W.: Asynchronous Holocene optimum of the East Asian monsoon, *Quat. Sci. Rev.*, 19, 743–762, 2000.
- 5 Berger, A.: Long-term variations of daily insolation and Quaternary climate changes, *J. Atmos. Sci.*, 35(12), 2362–2367, 1978.
- Braconnot, P., Marti, O., Joussaume, S., and Leclainche, Y.: Ocean feedback in response to 6 kyr BP insolation, *J. Climate*, 13, 1537–1553, 2000.
- Broström, A., Coe, M., Harrison, S. P., Gallimore, R., Kutzbach, J. E., Foley, J. A., Prentice, I. C., and Behling, P.: Land surface feedbacks and palaeomonsoons in northern Africa, *Geophys. Res. Lett.*, 25(19), 3615–3618, 1998.
- 10 Brovkin, V., Raddatz, T., Reick, C. H., Claussen, M., and Gayler, V.: Global biogeophysical interactions between forest and climate, *Geophys. Res. Lett.*, 36, L07405, doi:10.1029/2009GL037543, 2009.
- 15 Claussen, M.: Modelling bio-geophysical feedback in the African and Indian monsoon region, *Clim. Dynam.*, 13, 247–257, 1997.
- Claussen, M. and Gayler, V.: The greening of Sahara during the mid-Holocene: Results of an interactive atmosphere–biome model, *Global Ecol. Biogeogr.*, 6, 369–377, 1997.
- Clift, P. D. and Plumb, R. A.: *The Asian Monsoon: Causes, History and Effects*, Cambridge Univ. Press, Cambridge, 270 p., 2008.
- 20 Cui, X., Graf, H. F., Langmann, B., Chen, W., and Huang, R.: Climate impacts of anthropogenic land use changes on the Tibetan Plateau, *Global Planet. Change*, 54, 33–56, 2006.
- Diffenbaugh, N. S. and Sloan, L. C.: Global climate sensitivity to land surface change: The mid Holocene revisited, *Geophys. Res. Lett.*, 29(10), 1476, doi:10.1029/2002GL014880, 2002.
- 25 Ge, Q., Wang, S., Wen, Y., Shen, C., and Hao, Z.: Temperature and precipitation changes in China during the Holocene, *Adv. Atmos. Sci.*, 24(6), 1024–1036, 2007.
- Hales, K., Neelin, J. D., and Zeng, N.: Interaction of Vegetation and Atmospheric dynamical mechanisms in the mid-Holocene African monsoon, *J. Climate*, 19, 4105–4120, 2006.
- Harrison, S. P., Jolly, D., Laarif, F., Abe-Ouchi, A., Dong, B., Herterich, K., Hewitt, C., Joussaume, S., Kutzbach, J. E., Mitchel, J., De Noblet, N., and Valdes, P.: Intercomparison of simulated global vegetation distributions in response to 6 kyr BP orbital forcing, *J. Climate*, 11, 2721–2742, 1998.
- 30

Holocene climate change in Central and Eastern Asia

A. Dallmeyer et al.

Title Page

Abstract

Introduction

Conclusions

References

Tables

Figures



Back

Close

Full Screen / Esc

Printer-friendly Version

Interactive Discussion



- He, J., Ju, J., Wen, Z., Lü, J., and Jin, Q.: A review of recent advances in Research on Asian monsoon in China, *Adv. Atmos. Sci.*, 24, 6, 972–992, 2007.
- Herzschuh, U., Winter, K., Wünnemann, B., and Li, S.: A general cooling trend on the central Tibetan Plateau throughout the Holocene recorded by the Lake Zigetang pollen spectra, *Quat. Int.*, 154–155, 113–121, 2006.
- Herzschuh, U., Kramer, A., Mischke, S., and Zhang, C.: Quantitative climate and vegetation trends since the late glacial on the northeastern Tibetan Plateau deduced from Koucha Lake pollen spectra, *Quat. Res.*, 71, 162–171, 2009.
- Hewitt, C. D. and Mitchell, J. F. B.: A fully-coupled GCM simulation of the climate of the mid-Holocene, *Geophys. Res. Lett.*, 25, 361–364, 1998.
- Irizarry-Ortiz, M., Wang, G., and Elthair, E. A. B.: Role of the biosphere in the mid-Holocene climate of West Africa, *J. Geophys. Res.*, 108(D2), 4042, doi:10.1029/2001JD000989, 2003.
- Jolly, D., Prentice, I. C., Bonnefille, R., Ballouche, A., Bengo, M., Brenac, P., Buchet, G., Burney, D., Cazet, J. P., Cheddadi, R., Ector, T., Elenga, H., Elmoutaki, S., Guiot, J., Laarif, F., Lamb, H., Lezine, A. M., Maley, J., Mbenza, M., Peyron, O., Reille, M., Reynaud-Farrera, I., Riollet, G., Ritchie, J. C., Roche, E., Scott, L., Ssemmanda, I., Straka, H., Umer, M., Van Campo, E., Vilimumbalo, S., Vincens, A., and Waller, M.: Biome reconstruction from pollen and plant macrofossil data for Africa and the Arabian peninsula at 0 and 6000 years, *J. Biogeogr.*, 25, 6, 1007–1027, 1998.
- Joussaume, S. and Braconnot, P.: Sensitivity of paleoclimate simulations results to season definitions, *J. Geophys. Res.*, 102(D2), 1943–1956, 1997.
- Joussaume, S., Taylor, K. E., Braconnot, P., Mitchell, J. F. B., Kutzbach, J. E., Harrison, S. P., Prentice, I. C., Broccoli, A. J., Abe-Ouchi, A., Bartlein, P. J., Bonfils, C., Dong, B., Guiot, J., Herterich, K., Hewitt, C. D., Jolly, D., Kim, J. W., Kislov, A., Kitoh, A., Loutre, M. F., Masson, V., McAvaney, B., McFarlane, N., deNoblet, N., Peltier, W. R., Peterschmitt, J. Y., Pollard, D., Rind, D., Royer, J. F., Schlesinger, M. E., Syktus, J., Thompson, S., Valdes, P., Vettoretti, G., Webb, R. S., and Wyputta, U.: Monsoon changes for 6000 years ago: Results of 18 simulations from the Paleoclimate Modeling Intercomparison Project (PMIP), *Geophys. Res. Lett.*, 26(7), 859–862, 1999.
- Jungclaus, J. H., Botzet, M., Haak, H., Keenlyside, N., Luo, J.-J., Latif, M., Marotzke, J., Mikolajewicz, U., and Roeckner, E.: Ocean circulation and tropical variability in the coupled model ECHAM5/MPI-OM, *J. Climate*, 19, 3952–3972, 2006.
- Kohfeld, K. E. and Harrison, S. P.: How well can we simulate past climates? Evaluating the

Holocene climate change in Central and Eastern Asia

A. Dallmeyer et al.

Title Page

Abstract

Introduction

Conclusions

References

Tables

Figures

◀

▶

◀

▶

Back

Close

Full Screen / Esc

Printer-friendly Version

Interactive Discussion



Holocene climate change in Central and Eastern Asia

A. Dallmeyer et al.

Title Page

Abstract

Introduction

Conclusions

References

Tables

Figures

◀

▶

◀

▶

Back

Close

Full Screen / Esc

Printer-friendly Version

Interactive Discussion



- models using global palaeo-environmental data sets, *Quat. Sci. Rev.*, 19, 321–346, 2000.
- Kutzbach, J. E. and Otto-Bliesner, B.: The sensitivity of the African-Asian monsoonal climate to orbital parameter changes for 9000 yr BP in a low-resolution general circulation model, *J. Atmos. Sci.*, 39, 1177–1188, 1982.
- 5 Kutzbach, J. E. and Liu, Z.: Oceanic feedback on the western African monsoon at 6000 BP, *Science*, 278, 440–443, 1997.
- Lau, K.-M., Kim, K.-M., and Yang, S.: Dynamical and boundary forcing characteristics of regional components of the Asian summer monsoon, *J. Climate*, 13, 2461–2482, 2000.
- Levis, S., Bonan, G. B., and Bonfils, C., 2004: Soil feedback drives the mid-Holocene North African monsoon northward in fully coupled CCSM2 simulations with a dynamic vegetation model, *Clim. Dynam.*, 23, 791–802, 2004.
- 10 Li, Y. and Harrison, S.: Simulations of the impact of orbital forcing and ocean on the Asian summer monsoon during the Holocene, *Global Planet. Change*, 60, 505–522, 2008.
- Li, Y., Harrison, S., Zhao, P., and Ju, J.: Simulations of the impact of dynamic vegetation on interannual and interdecadal variability of Asian summer monsoon with modern and mid-Holocene orbital forcings, *Global Planet. Change*, 66(3/4), 235–252, 2009.
- 15 Liu, Y., Qing, B., Duan, A., Qian, Z., and Wu, G.: Recent progress in the impact of the Tibetan Plateau on climate in China, *Adv. Atmos. Sci.*, 24(6), 1060–1076, 2007.
- Liu, Z., Harrison, S. P., Kutzbach, J. E., and Otto-Bliesner, B.: Global monsoons in the mid-Holocene and oceanic feedback, *Clim. Dynam.*, 22, 157–182, 2004.
- 20 Maher, B. A.: Holocene variability of the East Asian summer monsoon from Chinese cave records: a re-assessment, *The Holocene*, 18(6), 861–866, 2008.
- Ohgaito, R. and Abe-Ouchi, A.: The role of ocean thermodynamics and dynamics in Asian summer monsoon changes during the mid-Holocene, *Clim. Dynam.*, 29, 39–50, 2007.
- 25 Otto, J., Raddatz, T., Claussen, M., Brovkin, V., and Gayler, V.: Separation of atmosphere-ocean-vegetation feedbacks and synergies for mid-Holocene climate, *Geophys. Res. Lett.*, 36, L09701, doi:10.1029/2009GL037482, 2009.
- Raddatz, T. J., Reick, C. H., Knorr, W., Kattge, J., Roeckner, E., Schnur, R., Schnitzler, K.-G., Wetzels, P., and Jungclaus, J.: Will the tropical land biosphere dominate the climate-carbon cycle feedback during the twenty-first century?, *Clim. Dynam.*, 29, 565–574, 2007.
- 30 Ren, G.: Changes in forest cover in China during the Holocene, *Veg. Hist. Archaeobot.*, 16, 119–126, 2007.
- Ren, G. and Beug, H.-J.: Mapping Holocene pollen data and vegetation of China, *Quat. Sci.*

Rev., 21, 1395–1422, 2002.

Roeckner, E., Bäuml, G., Bonaventura, L., Brokopf, R., Esch, M., Giorgetta, M., Hagemann, S.,
Kirchner, I., Kornblueh, L., Manzini, E., Rhodin, A., Schlese, U., Schultzweida, U., and Tomp-
kins, A.: The atmospheric general circulation model ECHAM5. Part I: Model description,
5 MaxPlanckInst. f. Meteor., Report No. 349, Hamburg, 2003.

Roeckner, E., Brokopf, R., Esch, M., Giorgetta, M., Hagemann, S., Kornblueh, L., Manzini, E.,
Schlese, U., and Schulzweida, U.: Sensitivity of simulated climate to horizontal and vertical
resolution in the ECHAM5 atmosphere model, *J. Climate*, 19, 3771–3791, 2006.

Shen, J., Jones, R. T., and Yang, X.: The Holocene vegetation history of Lake Erhai, Yunnan
10 province, southwestern China: the role of climate and human forcings, *The Holocene*, 16,
265–276, 2006.

Tang, L., Shen, C., Liu, K., and Overpeck, J. T.: New high resolution pollen records from two
lakes in Xizang (Tibet), *Acta Bot. Sin.*, 41, 896–902, 1999.

Texier, D., de Noblet, N., and Braconnot, P.: Sensitivity of the African and Asian monsoons to
15 mid-Holocene insolation and data-inferred surface changes, *J. Climate*, 13, 164–181, 2000.

Voss, R. and Mikolajewicz, U.: The climate of 6000 years BP in near-equilibrium simulations
with a coupled AOGCM, *Geophys. Res. Lett.*, 28(11), 2213–2216, 2001.

Wang, H.-J.: Role of vegetation and soil in the Holocene megathermal climate over China, *J.*
Geophys. Res., 104(D8), 9361–9367, 1999.

20 Webster, P. J., Magaa, V. O., Palmer, T. N., Shukla, J., Tomas, R. A., Yanai, M., and Yasunari, T.:
Monsoons: Processes, predictability, and the prospects for prediction, *J. Geophys. Res.*,
103(C7), 14451–14510, 1998.

Wei, J. and Wang, H.: A possible role of solar radiation and ocean in the mid-Holocene East
Asian monsoon Climate, *Adv. Atmos. Sci.*, 21(1), 1–12, 2004.

25 Wu, G., Liu, Y., Wang, T., Wan, R., Liu, X., Li, W., Wang, Z., Zhang, Q., Duan, A., and Liang, X.:
The influence of mechanical and thermal forcing by the Tibetan Plateau in Asian climate, *J.*
Hydrometeorol., 8, 770–789, 2007.

Yasunari, T., Saito, K., and Takata, K.: Relative roles of large-scale orography and land surface
30 processes in the global hydroclimate. Part 1: Impacts on monsoon systems and the Tropics,
J. Hydrometeorol., 7, 626–641, 2006.

Yu, G., Chen, X., Ni, J., Cheddadi, R., Guiot, J., Han, H., Harrison, S., Huang, C., Ke, M.,
Kong, Z., Li, S., Li, W., Liew, P., Liu, G., Liu, J., Liu, Q., Liu, K.-B., Prentice, I. C., Ren, G.,
and Qui, W.: Palaeovegetation of China: a pollen data-based synthesis for the mid-Holocene

Holocene climate change in Central and Eastern Asia

A. Dallmeyer et al.

Title Page

Abstract

Introduction

Conclusions

References

Tables

Figures

◀

▶

◀

▶

Back

Close

Full Screen / Esc

Printer-friendly Version

Interactive Discussion



- and last glacial maximum, *J. Biogeogr.*, 27, 635–664, 2000.
- Zhao, Y., Yu, Z., and Chen, F.: Spatial and temporal patterns of Holocene vegetation and climate changes in arid and semi-arid China, *Quat. Int.*, 194, 6–18, 2009.
- 5 Zheng, Y. Q., Yu, G., Wang, S. M., Xue, B., Zhuo, D. Q., Zeng, X. M., and Liu, H. Q.: Simulation of paleoclimate over East Asia at 6 ka BP and 21 ka BP by regional climate model, *Clim. Dynam.*, 23, 513–529, 2004.

CPD

5, 2351–2389, 2009

Holocene climate change in Central and Eastern Asia

A. Dallmeyer et al.

Title Page

Abstract

Introduction

Conclusions

References

Tables

Figures



Back

Close

Full Screen / Esc

Printer-friendly Version

Interactive Discussion



Holocene climate change in Central and Eastern Asia

A. Dallmeyer et al.

Table 1. Start day and length of the seasons for the mid-Holocene and present-day orbital configuration, respectively. The seasons are defined on astronomical calendar, based on the time of vernal and autumnal equinox as well as summer and winter solstice. The beginning of the seasons is shifted backwards by three weeks.

Season	6 k		0 k	
	Start (day)	Length (days)	Start (day)	Length (days)
Winter	334	93	336	88
Spring	62	94	59	93
Summer	156	89	152	94
Autumn	245	89	246	90

Title Page

Abstract

Introduction

Conclusions

References

Tables

Figures

◀

▶

◀

▶

Back

Close

Full Screen / Esc

Printer-friendly Version

Interactive Discussion



Table 2. Description of the areas we consider in our feedback study. Listed are the abbreviation, geographic position (latitude and longitude of grid-box centers) as well as a short characterization. The areas are formed, based on topography and on the simulated Holocene vegetation trend. Regions marked with an asterisk (*) are modified and do not completely contain all grid-boxes in the mentioned geographic areas (see Fig. 1).

Region	Longitude (° E)	Latitude (° N)	Description
IND*	71.25–78.75	12.99–24.12	Indian subcontinent (land only), core region Indian monsoon
INCPIN*	93.75–108.75	12.99–20.41	Indochina Peninsula (land only), tropical region, influenced by East Asian monsoon
PAK	56.25–75	27.83–31.55	Includes parts of Pakistan, Afghanistan and Iran, affected by the Indian monsoon
BENG	82.5–97.5	24.12–27.83	Northern coast of the Bay of Bengal, includes Ganges and Brahmaputra river valleys, and parts of Himalaya, influenced by Indian monsoon
TP*	75–101.25	27.83–38.97	Tibetan Plateau (model orography higher than 2500 m), affected by Indian and East Asian monsoon
YANG	105–120	31.54–38.97	Yangtze and Huanghe plain, represents core region of the East Asian monsoon
DES	63.75–90	42.68–46.39	Desert and steppe area south of the Lake Balkhash, influenced by mid-latitude westerlies
EASM*	93.75–108.75	38.97–46.38	Margin area of the East Asian summer monsoon, includes parts of the Gobi desert
RUS	86.25–101.25	50.10–53.81	Russia, northern margin of the Altai Mountains, represents mid-latitude, vegetated area outside the monsoon region
NECH	116.25–135	46.39–53.81	Northeastern China, lower reaches of the Amur river, might be affected by East Asian monsoon
CETP	82.5–97.5	35.26–38.97	Control region on the central Tibetan Plateau, region with strongest vegetation dynamic

Holocene climate change in Central and Eastern Asia

A. Dallmeyer et al.

Title Page

Abstract

Introduction

Conclusions

References

Tables

Figures



Back

Close

Full Screen / Esc

Printer-friendly Version

Interactive Discussion



Holocene climate change in Central and Eastern Asia

A. Dallmeyer et al.

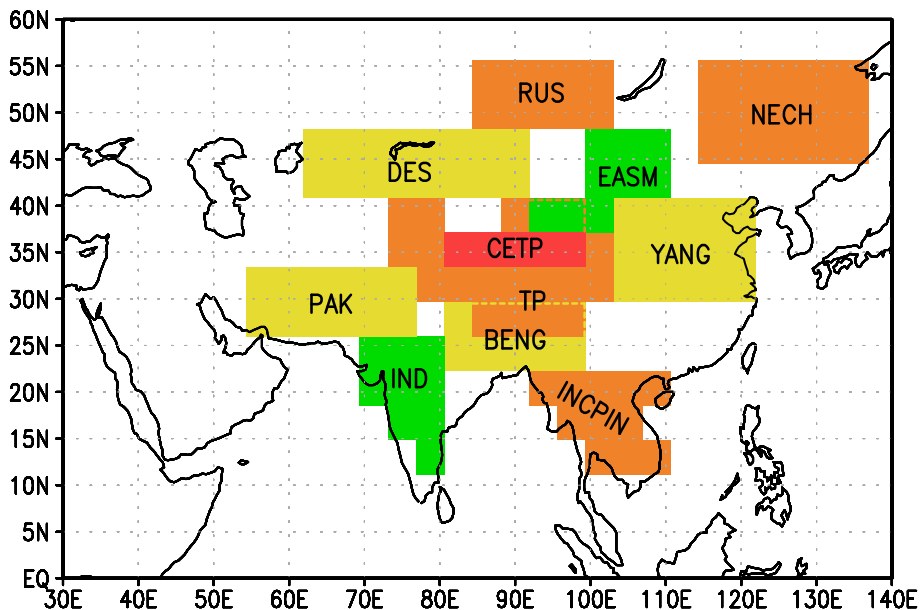


Fig. 1. Location of the areas we consider in our feedback study. Dashed lines mark the border of regions, which overlap with other areas. The areas are formed, based on topography and on the simulated Holocene vegetation trend.

Title Page

Abstract

Introduction

Conclusions

References

Tables

Figures

◀

▶

◀

▶

Back

Close

Full Screen / Esc

Printer-friendly Version

Interactive Discussion



Holocene climate change in Central and Eastern Asia

A. Dallmeyer et al.

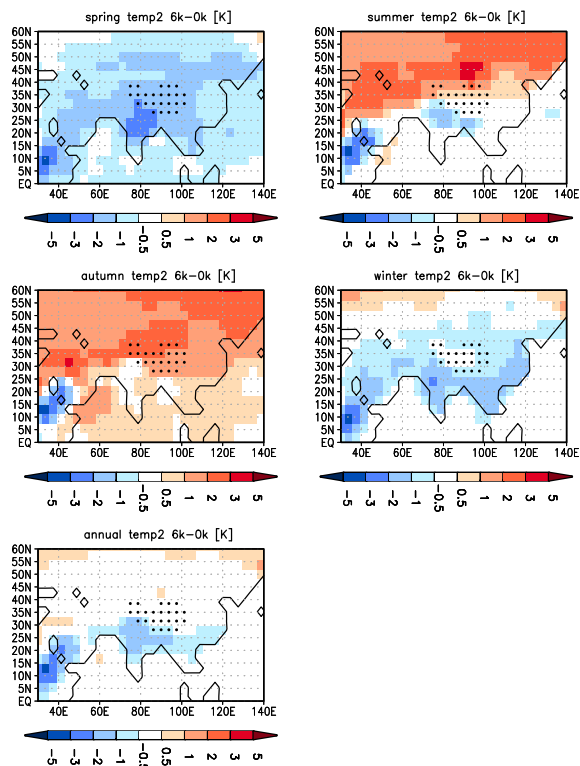


Fig. 2. Seasonal and annual averaged 2 m-temperature anomalies (K) between mid-Holocene and present-day according to the coupled experiment AOV. Seasons are defined on astronomical calendar, based on the time of vernal and autumnal equinox and summer and winter solstice. The annual temperature anomaly is calculated on daily model output. Due to the different length of the respective seasons in 6 k and 0 k, the annual mean value is not the arithmetic average of the seasons. Stippled area indicates the Tibetan Plateau (orography in the model higher than 2500 m).

Title Page

Abstract

Introduction

Conclusions

References

Tables

Figures

◀

▶

◀

▶

Back

Close

Full Screen / Esc

Printer-friendly Version

Interactive Discussion



Holocene climate change in Central and Eastern Asia

A. Dallmeyer et al.

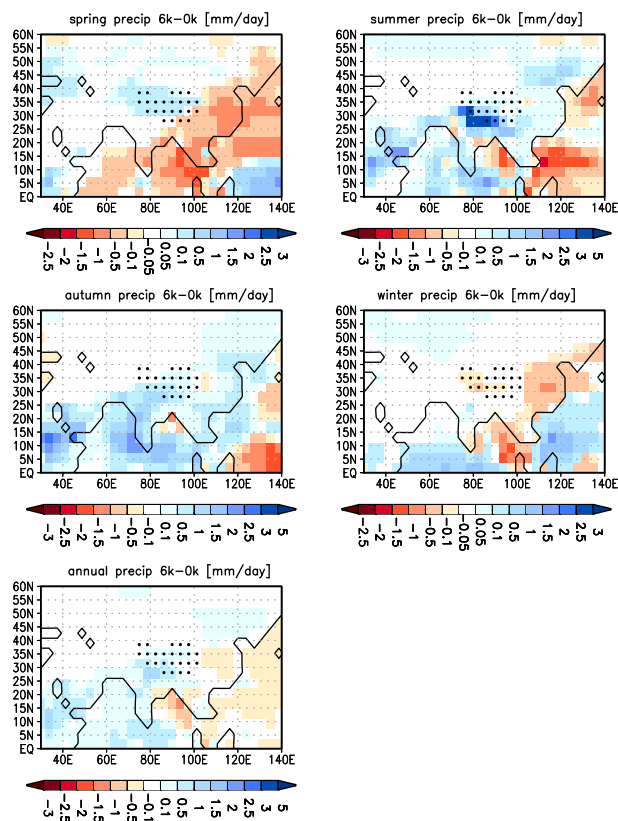


Fig. 3. Same as Fig. 2, but for seasonal and annual averaged precipitation anomalies (mm/d). One has to be careful with the interpretation of precipitation changes. Due to the differences in the length of the respective seasons between 6 k and 0 k, a higher precipitation rate per day does not necessarily indicate a higher seasonal mean, i.e. a higher amount of precipitation per season. Please note the change in colour scales.

Title Page

Abstract

Introduction

Conclusions

References

Tables

Figures

◀

▶

◀

▶

Back

Close

Full Screen / Esc

Printer-friendly Version

Interactive Discussion



Holocene climate change in Central and Eastern Asia

A. Dallmeyer et al.

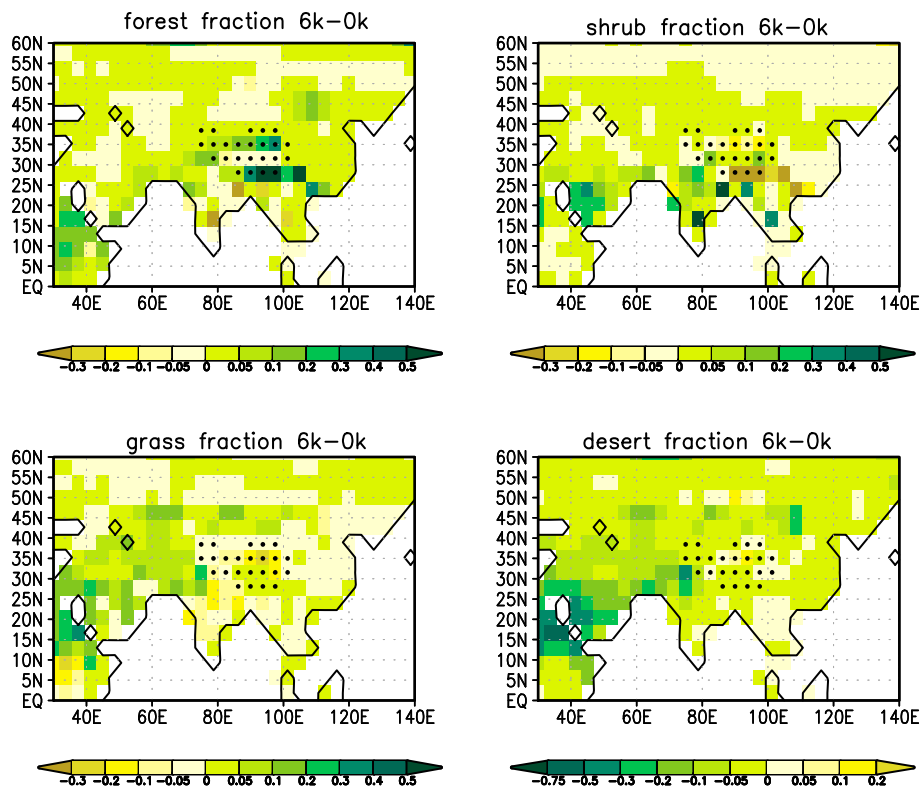


Fig. 4. Simulated land cover change between mid-Holocene and present-day, given as fraction of forest, shrubs, grass and non-vegetated area (referred to as desert) per grid-box. Stippled area indicates the Tibetan Plateau (orography in the model higher than 2500 m). Please note the change in colour scales.

[Title Page](#)[Abstract](#)[Introduction](#)[Conclusions](#)[References](#)[Tables](#)[Figures](#)[◀](#)[▶](#)[◀](#)[▶](#)[Back](#)[Close](#)[Full Screen / Esc](#)[Printer-friendly Version](#)[Interactive Discussion](#)

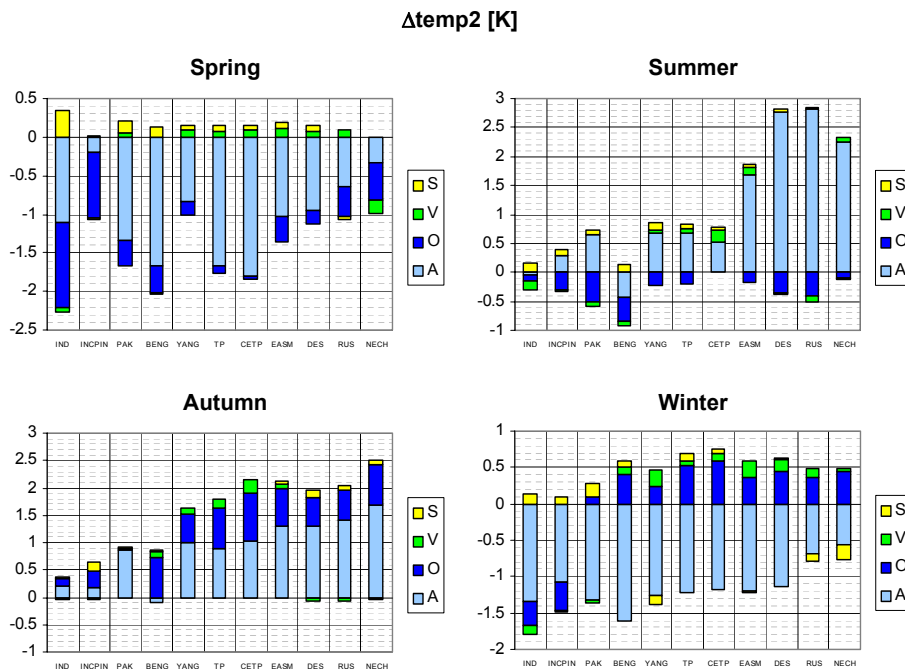


Fig. 5. Factors contributing to the seasonal temperature change between mid-Holocene (6 k) and present-day for 11 regions in Central and Eastern Asia. Seasons are defined on astronomical calendar, based on the time of vernal and autumnal equinox as well as summer and winter solstice. Light blue colours show the results of the atmosphere-only run, i.e. the direct response of atmospheric dynamics (A) to changes in insolation. Dark blue colours represent the contribution of ocean–atmosphere-interaction (O), including sea-ice dynamics. Green colours indicate the contribution of vegetation–atmosphere interaction (V). Yellow colours reveal the contribution of the synergy (S) between atmosphere–ocean and atmosphere–vegetation feedback. Please note the change in scales.

[Title Page](#)
[Abstract](#)
[Introduction](#)
[Conclusions](#)
[References](#)
[Tables](#)
[Figures](#)

[Back](#)
[Close](#)
[Full Screen / Esc](#)
[Printer-friendly Version](#)
[Interactive Discussion](#)


Holocene climate change in Central and Eastern Asia

A. Dallmeyer et al.

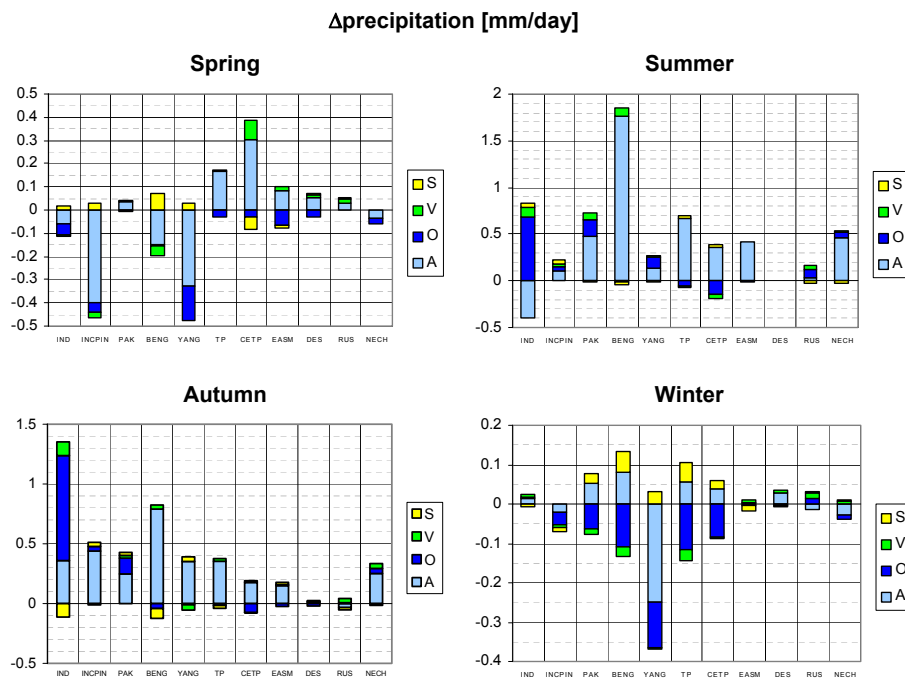


Fig. 6. Same as Fig. 5, but for precipitation anomalies (mm/d). Please note the change in scales.

Title Page

Abstract

Introduction

Conclusions

References

Tables

Figures

⏪

⏩

◀

▶

Back

Close

Full Screen / Esc

Printer-friendly Version

Interactive Discussion



Holocene climate change in Central and Eastern Asia

A. Dallmeyer et al.

Title Page

Abstract

Introduction

Conclusions

References

Tables

Figures

◀

▶

◀

▶

Back

Close

Full Screen / Esc

Printer-friendly Version

Interactive Discussion

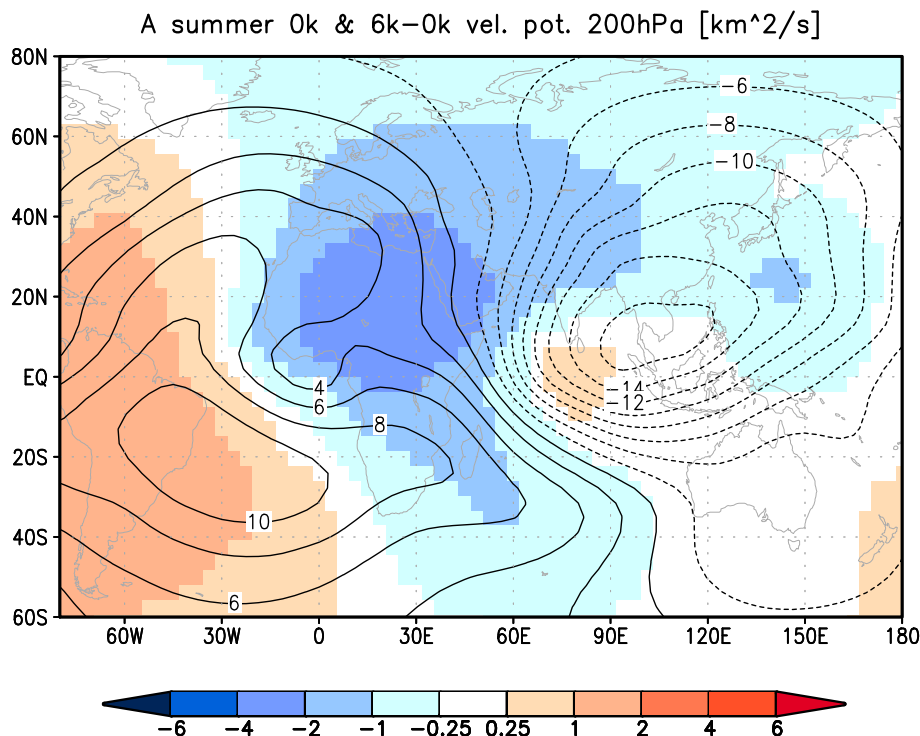


Fig. 7. Upper-tropospheric velocity-potential (200 hPa, km^2/s) as simulated by the atmosphere-only model, averaged over the summer season. Contour lines illustrate the velocity-potential under present-day orbital configuration. Shaded areas show the velocity-potential anomalies between 6 k and 0 k. Negative values represent divergence, positive values convergence.

Holocene climate change in Central and Eastern Asia

A. Dallmeyer et al.

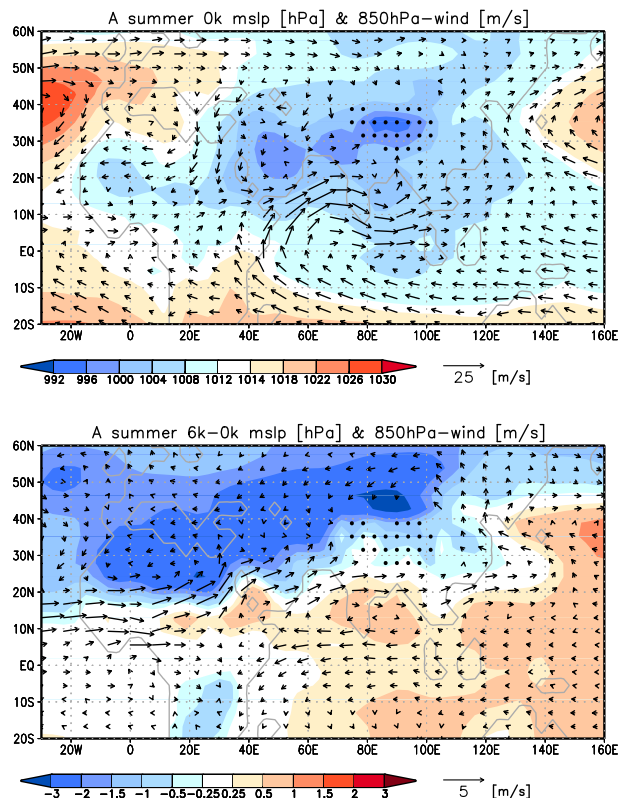


Fig. 8. Summer mean sea level pressure (shaded, hPa) and wind in 850 hPa (vector, m/s) as simulated by the atmosphere-only model. Upper panel: present-day (0k), lower panel: anomalies between 6k and 0k. Stippled areas mark the Tibetan Plateau (orography in the model higher than 2500 m). No wind vectors are shown, where the orography in the model exceeds 1500 m (approximately corresponding to the 850 hPa-Niveau).

[Title Page](#)[Abstract](#)[Introduction](#)[Conclusions](#)[References](#)[Tables](#)[Figures](#)[◀](#)[▶](#)[◀](#)[▶](#)[Back](#)[Close](#)[Full Screen / Esc](#)[Printer-friendly Version](#)[Interactive Discussion](#)

Holocene climate change in Central and Eastern Asia

A. Dallmeyer et al.

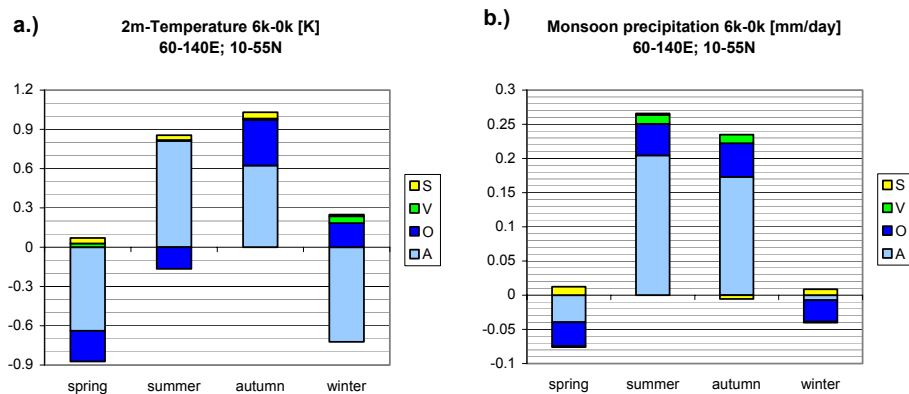


Fig. 9. Same as Fig. 5, but as regional (60–140° E, 10–55° N) averages for **(a)** temperature (left panel) and **(b)** precipitation (right panel). Only grid-points on land are taken into account.

Title Page

Abstract

Introduction

Conclusions

References

Tables

Figures

◀

▶

◀

▶

Back

Close

Full Screen / Esc

Printer-friendly Version

Interactive Discussion

